An investigation of photo-activation of psoralen (AMT) during radiation therapy in a novel tissue model

by

Russell Patrick Holden

Department of Medical Physics
Duke University

Date:_____
Approved:

_____
Mark Oldham, Advisor

_____
Scott Floyd

_____
Justus Adamson

Thesis submitted in partial fulfillment of
the requirements for the degree of Master of Science in the Department of
Medical Physics in the Graduate School
of Duke University

2021

ABSTRACT

An investigation of photo-activation of psoralen (AMT) during radiation therapy in a novel tissue model

by

Russell Patrick Holden

Department of Medical Physics
Duke University

Date:_____
Approved:

_____
Mark Oldham, Advisor

_____
Scott Floyd

_____
Justus Adamson

An abstract of a thesis submitted in partial fulfillment of the requirements for the degree of Master of Science in the Department of Medical Physics in the Graduate School of Duke University

2021

# Abstract

**Purpose:** RECA (Radiotherapy Enhanced by Cherenkov photo-Activation) is a novel treatment with potential to add an anti-cancer immunogenic component through Cherenkov activation of a photo-chemotherapeutic agent (psoralen). This work investigates RECA in a novel tissue-representative in-vitro model consisting of 4T1 murine cancer cells grown on thin slices of viable rat-brain tissue.

**Methods:** Accurate estimation of viable tumor burden is of foundational importance to this work. A CellProfiler pipeline was created, optimized and validated on realistic simulated data/images where the ground truth of number of colonies and integrated intensity was known. Simulated data sets mimicked key features of real experimental data including colony spatial and size distributions, contaminant and stray light signals, colony overlap, and noise. The optimized CellProfiler pipeline was then applied to the original 4T1 tumor cell images to determine colony growth over five days.

Several experiments were conducted prior to the RECA experiment to determine the best protocol. The first tested the optimal concentration of psoralen, loading technique, and type of psoralen by co-incubating 4T1 cells with psoralen for differing times and concentrations and subsequently exposing them to 365nm radiation at variable energy fluences. The plates were tested for 4T1 cell viability using Celltiter-glo and luciferase assay 48-72 hours later depending on confluence of the control plate.

Another experiment tested the output of the CellProfiler image analysis for relative growth over time measuring 4T1 mCherry cells plated on rat brain slices at 10k,20k,30k,40k,50k cells per hemisphere.

For the RECA experiment, six 12-well plates, each containing 1cm of agarose supporting a 400 μm thick coronal slice of viable rat brain tissue were created. Each plate represented one arm of an experiment incorporating the psoralen derivative 4'-aminomethyl trioxsalen (AMT): MV control, MV+AMT, kV control, kV+AMT, no irradiation control, and AMT alone control. 20,000 4T1 cells expressing both mCherry-flourescent and firefly luciferase-luminescent reporter proteins plated on each rat brain slice hemisphere. For the AMT arms, the cells were co-incubated with 1 μM AMT for 1 hour prior to plating. The MV arms received 4 Gy from a 15 MV linear accelerator beam, and the kV arms received 4 Gy from 160 keV photons. Images were taken of the plates each day for 5 days with a Zeiss Lumar microscope with rhodamine filter for the mCherry protein signal.

**Results:** The CellProfiler pipeline measured integrated intensity of the 10 simulated images that best approximated the images from the experiment with an accuracy of 99.23% ± 0.75%. Further analysis on images with increasing colonies, background, and noise showed the pipeline was accurate on images with variable features. These results gave confidence that the same pipeline could be used on images from this experiment.

AMT was found to be a more effective psoralen (0.43 ± 0.22% cell survival after 48hr) relative to 8-MOP (31.3% ± 3.7% cell survival after 72hr). The psoralen cell loading was found to be optimal at 1μM for 1 hr prior to plating. The analysis of the cell titration images showed a significant increase in signal for each increase in cells plated on day one and for all subsequent days except for the 20k cell arm. Additionally, the growth in signal for the plates was consistent between the arms except for the 20k arm due to extra signal on the periphery of the slice likely from displaced cells.

Integrated intensity analysis of the 4T1 mCherry cells revealed a significant decrease in tumor proliferation by day 5 between the MV control (5.65±0.78-fold growth) and MV AMT (3.49±-0.52-fold growth) arms. This result is consistent with the hypothesis that psoralen is being activated, causing the decreased proliferation seen in MV AMT arm. The kV control and kV AMT arms had a smaller decrease in proliferation when compared to their MV counterparts (6.73±1.24 and 5.26±0.59-fold growth respectively). The growth observed in the Dark control arm was consistent with the 13.6 ± 1.5 hour doubling time for 4T1 cells. In the MV AMT arm, there were punctuated regions of increased signal in 7/12 wells not corresponding to colonies, making segmentation for this arm challenging. The viability of the brain slice was assessed each day and found to be stable over the 5 days.

**Conclusions:** The technique of testing image analytic software on simulated images proved to be an effective tool to verify the software's accuracy. A similar technique can be applied to images with new and challenging features.

The rat brain slice model gives the opportunity to both generate Cherenkov in real tissue while providing a 3D matrix for the colonies to grow, which is an improvement to the 2D well plate culture for this experiment. This new model adds challenges of proper image analysis with cell autofluorescence as well as cell clumping.

The preliminary results are consistent with psoralen activated in RECA treated cells causing decreased proliferation for the MV arm. Further work is needed to confirm and quantify the effect.

# Contents

## List of Figures

# Acknowledgments

*Mark Oldham, PhD*

*Jun Hyung Park*

*Anna Lynnette Price*

*Denise Dunn*

*Scott Floyd, MD, PhD*

*Justus Adamson, PhD*

# 1. Introduction

## *1.1 Psoralen*

Psoralen is a naturally occurring molecule belonging to the furanocoumarin family, and is found in citrus fruits, parsley, celery, fig. Psoralen is clinically approved to treat psoriasis, vitiligo, cutaneous T-cell lymphoma, graft-versus-host disease, and the reduction of pathogens in blood for blood transfusion[1,2,3]. The mechanism of action of psoralen involves the psoralen molecule diffusing across the lipid bilayer of cells and subsequently traveling into the nucleus, and the planar structure of the psoralen allows it to intercalate with the DNA[4]. Prior to the activation of psoralen, the molecule is mostly inert. Following activation by a photon within a specific energy range (predominately UVA), the psoralen molecule covalently binds 5′-TpA-3′ sites in DNA[5]. This first activation forms a 4′,5′- monoadduct. Absorption of a second photon causes the 3,4 site to double bond to another thymine base. These two bonds form a crosslink between the two DNA strands. These monoadducts and crosslinks are the purported cause of the immunogenic effects seen in cancer cells treated with psoralen[5]. These effects include up-regulation of major histocompatibility complex I (MHC I), up-regulation of immunogenic transcription factors, and promotion of T-cell development, maturation, and proliferation[6].

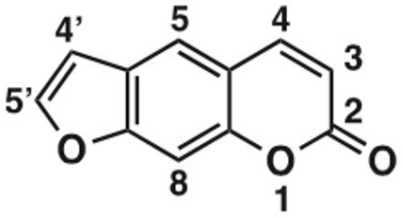


**Figure 1: Psoralen numbering scheme[5]**

The function of psoralen is dependent on UVA activation, and UVA photons have a depth of penetration of roughly 1mm, limiting psoralen to superficial treatments. Given the immunogenic systemic wide effect seen in photoactivated psoralen treatments, activation of psoralen in a non-superficial tumor may have similar results.

## *1.2 X-PACT*

One method that has been shown to have potential for treating deeper tumors is called X-PACT (X-Ray Psoralen Activated Cancer Therapy)[7]. This method utilizes co-incubating phosphors with psoralen and injecting the combination into the tumor. The location is irradiated with KV X-rays to activate the phosphor, which absorbs the X-ray and re-emits lower energy photons, predominately within UVA spectrum. This UVA light then activates the psoralen. This method has been shown to be effective in both in-vitro and in-vivo applications[7].

X-PACT was tested in-vitro on 4T1-HER2 cells treated with UVADEX (8-MOP), phosphor and 1 Gy of 80 kVp X-rays. There was a significant increase in cytotoxicity for the arm treated with with 8-MOP and phosphor receiving X-rays relative to cells receiving X-rays alone[7]. This increase in cytotoxicity is suggestive that the psoralen

activation by the phosphor caused the increase in cytotoxicity. In addition, there was a linear relationship between increases in dose, psoralen concentration, phosphor concentration and an increase in cytotoxicity. Next, X-PACT was tested in-vivo on BALB/c mice with syngeneic 4T1-HER2 tumors and it was found that X-PACT treated mice had significantly slower tumor growth than with saline or AMT (4′-Aminomethyl-4,5′,8-trimethylpsoralen) + X-ray[7].

## *1.3 Scope*

The results from kV X-PACT have been promising to-date; however, the approach has several inherent limitations, including uncertain biological effects and toxicities of the phosphors, and the reliance on kV irradiation with associated poor depth penetration and high bone dose. To overcome these limitations, a novel method of activating psoralen called "Radiatiotherapy Enhanced with Cherenkov photoactivation" (RECA) was proposed[8]. In RECA treatment a clinical external beam radiation treatment is delivered to the tumor while concomitantly emitted Cherenkov light activates psoralen localized to the treatment area. Previous work has demonstrated the potential for RECA treatment efficacy, and this work examines the next step in testing this treatment utilizing a novel rat brain slice in-vitro model along with a rigorous image analysis technique[8].

## *1.4 Cherenkov Radiation*

Cherenkov radiation occurs when a charged particle moves faster than the phase velocity of light in a dielectric medium. The effect was first recorded by a scientist named Pavel Cherenkov[9].Cherenkov radiation is created by polarizations created in a dielectric medium by the moving charged particle. The polarized atoms subsequently depolarize and release photons that propagate out radially from the atom.

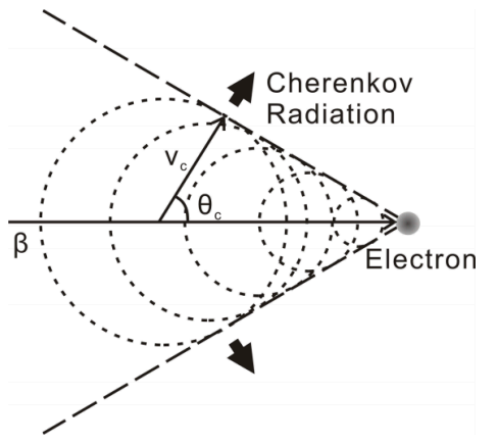


**Figure 2: Schematic of Cherenkov Emission[10]**

This Cherenkov light is incidentally created during external beam radiation therapy and can be used in dose verification and entrance/exit imaging[11]. In addition to imaging, testing on radiopharmaceuticals such as 18-FDG to generate Cherenkov within the patient and activate photosensitizers has shown promise[12]. The challenge with this method is that the magnitude of light generated is significantly less than other photoactivating techniques[13].

### 1.4.1 Prior RECA work

RECA (Radiotherapy Enhanced by Cherenkov photo-Activation) is a novel technique utilizing Cherenkov light generated during external beam radiation treatment to activate psoralen in deep tumors. Given that fluence of light is a limiting factor in activation of photosensitizers, Shrock *et al.* devised Monte Carlo simulations at different photon energies, dose rates, and filters to maximize the fluence of Cherenkov light[14]. It was found that higher energy beams, along with an aluminum filter to harden the beam, maximized Cherenkov light emissions.

In addition to fluence considerations, the activation of psoralen requires wavelengths specifically within the UVA range. The graph below illustrates the overlap between the relevant wavelength of Cherenkov light and Psoralen absorbance[14].

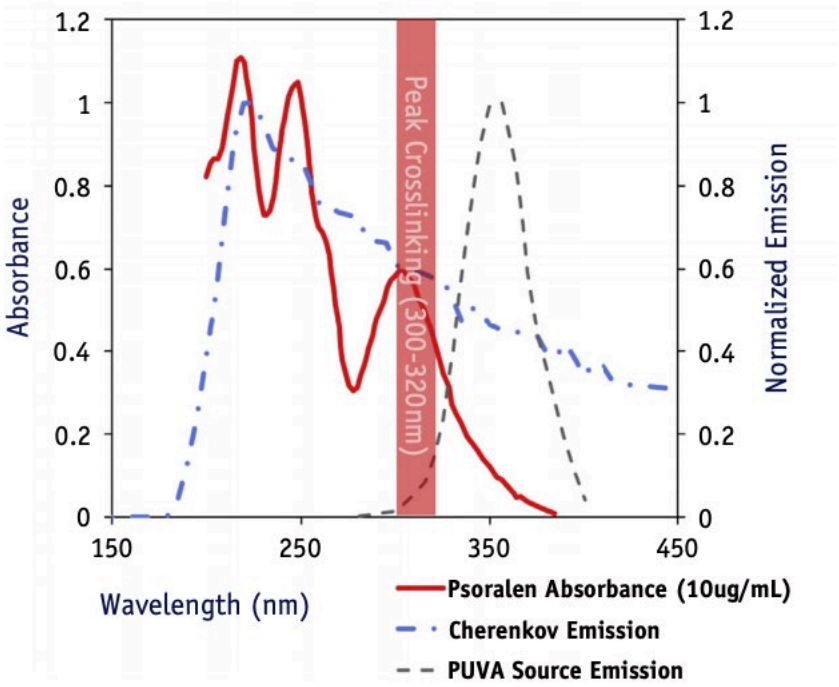


**Figure 3: Psoralen absorbance spectrum of 8-methoxypsoralen compared with Cherenkov emission from a 15-MV photon beam in water obtained using GEANT4/GAMOS Monte Carlo Simulations[14]. Additionally, a traditional PUVA light source emission distribution for comparison[8]. Significant overlap is seen within the peak crosslinking range of 300-320nm of Psoralen absorbance and Cherenkov emission.**

The overlap between Psoralen absorbance and Cherenkov emission in the Peak crosslinking 300-320nm range gives confidence that sufficient Cherenkov fluence should be able to activate Psoralen at the clinically relevant wavelength(Figure 3).

Yoon *et al.* conducted an experiment to corroborate the effect of beam energy on Chernkov light production[8]. This experiment used quinine to absorb the Cherenkov light generated from 6,10,15 MV beams within a water tank and measured the re-emitted blue light proportional to Cherenkov light absorbed. This study also found an

increase in Cherenkov light produced with higher energy as well as an increase using a low-Z filter such as aluminum[8].

In addition, this work conducted an in-vitro study to investigate the potential of radiotherapy plus RECA vs radiotherapy alone to increase cytotoxicity and increase expression of MHC I within B16 melanoma and 4T1 murine breast cancer cells[8]. This study utilized 3cm of solid water placed below the well plate to generate the Cherenkov light from a PA beam and a light block between the solid water and the well plate to prevent Cherenkov light from reaching the control wells. Following 2 Gy at 6MV, the cells receiving RECA had 20% and 9.5% increased cytotoxicity for 4T1 and B16 cells, respectively, compared with radiation and psoralen alone[8]. Also, well plates receiving RECA treatment had MHC I expression that was increased by 450% and 250% at 3 Gy and 6 Gy relative to psoralen and radiation alone. MHC I is a cell surface protein that presents proteins to the immune system and can cause an increased immune response. Finally, clonogenic studies using B16 cells showed a decrease in tumor viability by 7% and 36% at 6 and 12 Gy respectively for the RECA treated arms compared to psoralen and radiation alone[8].

This work gave evidence that Cherenkov light can activate psoralen and thereby increase cytotoxicity and upregulate MHC I. One limitation of the study was that solid water was used to generate the Cherenkov light and solid water was subsequently

found to have low Cherenkov light production relative to tissue as well as the potential to scintillate[16].

Inspired by the Yoon paper, subsequent work by Sagarika *et al.* quantified Cherenkov emissions from solid water, animal tissue, and agarose doped with different concentrations of india ink[15]. To do this, a high-sensitivity cooled camera equipped with UVA lenses and a filter was used to image samples irradiated with a 15MV beam. Lead blocks were placed to block the radiation from the linac head as well as other scatter not from the material itself. It was found that white solid water emitted 66 ± 5%, 64 ± 5% and 76 ± 3% less UVA than chicken breast, pork loin, and pork belly respectively. Additionally, it was found that 250ppm india ink emitted equivalent Cherenkov light to chicken breast (within 8%) which was taken to be human tissue equivalent[15].

Most recently, preliminary work by Xiangyu *et al.* [16] conducted a RECA experiment on 4T1 mCherry firefly luciferase murine mammary cancer cells using a novel rat brain slice in-vitro model. 4T1 cells were co-incubated with a 1mM 8-MOP solution prior to plating on rat brain slice hemispheres within a transwell insert. The cells were irradiated using a 15MV linear accelerator PA beam to deliver 4 Gy. The 2 cm thick Tissue equivalent-Cherenkov producing 250ppm india ink agarose was used to generate Cherenkov light beneath the rat brain slices receiving RECA. 2cm thick 1000ppm india ink agarose was used to absorb most Cherenkov light beneath the –

Cherenkov arms. Images were taken each day for 5 days using the Zeiss Lumar microscope with a rhodamine filter. In addition, a luciferase assay was done to quantify cell viability on day 5. The luciferase assay along with the image analysis did not find any statistically significant effects in the RECA arm and results were inconclusive.

One of the challenges in this experiment was the image analysis given the high and variable background, along with cell clumping. In preparation for a repeat of this experiment, an image analysis technique was developed to measure images with the challenging features seen in this experiment (Section 1.5).

## *1.5 Rat Brain Slice In-Vitro Technique*

Prior RECA experiments involved growing cancer cells in-vitro in standard well culture plates and irradiating them within the plate[7]. Standard well plates, where cells are cultured on agarose, may not be 'tissue-equivalent' or representative of real tissue from the perspective of mimicking similar Cherenkov generation because the optical properties of agarose gel and tissue are quite different. To better approximate an in-vivo assay, a Rat Brain Slice culture model were used in this experiment[17]. Organotypic brain slice models have been used extensively for their preservation of architecture and most cellular interactions[17]. In this work, organotypic rat brain slices were chosen not only to

create a 3D scaffold in which the cells can grow, but also to allow for Cherenkov light to be generated within tissue to simulate an in-vivo scenario. The rat brain slice allows Cherenkov light to be generated in 3D relative to the cells as opposed to directly below as is the case in a typical in-vitro experiment.

## *1.6 Image analysis technique*

Many fields, including microbiology, molecular biology, and immunology, require accurate measurements of the quantity of cells growing in well plates, cell morphology, and protein expression. The gold standard has been to manually count or segment prior to measuring the signal/colonies. However, when the sample size is large, it can become very challenging to measure these data sets due to time limitations and accurately applying the same analysis to each image. This necessitates the use of automated software. A variety of software are available including NIST[18] integrated counter, ChiTA[19], OpenCFU[20], ImageJ edge[21], CellProfiler[22], among others. Each software has its strengths and weaknesses depending on the data set used[21]. Modifying the inputs of the software algorithms for different datasets is essential and can have a profound impact on the output. For this study, CellProfiler was selected for its accuracy in measuring area and intensity of colonies, it's customizability, and also prior experience in the Floyd Lab[23].

The previous experiment testing RECA used rat brain slices as an in-vitro model to test Cherenkov activation[16]. 4T1 mCherry firefly luciferase cells were used and the

luminescence from the mCherry protein was measured as the metric for cell viability. The images from this experiment were challenging to analyze with a high level of background, cell autofluorescence, and clumping of colonies. Given the challenges of analyzing these images a technique was developed to test the CellProfiler pipeline. The technique was to create simulated images on MATLAB which approximate the experimental images. These images have known ground truth colony count, area, and intensity. CellProfiler is used to analyze these images, and the parameters for the pipeline were changed until it accurately measured the ground truth metrics. This optimized pipeline was then used to analyze the RECA experiment image set. For subsequent rat brain slice experiments with a similar setup, the same pipeline with small modifications was used.

## 2. A consistent, accurate, automated method for estimating viable tumor cell burden

The image analysis technique was developed as a CellProfiler pipeline that was tested using simulated images that approximated the images taken from the previous RECA experiment (Xiangyu *et al.* 2020)[16]. In this experiment, 10,000 4T1 mCherry firefly luciferase mouse mammary tumor cells were plated on 400 μm rat brain slices on top of transwell inserts within 6 well plates. Four total 6 well plates were used with 3 wells in each plate receiving 8-MOP and 3 DMSO control. The plates were divided into 4 arms– no irradiation, kV irradiation with 160 keV to 4 Gy, MV irradiation PA through 250ppm

doped agarose (light), and MV irradiation PA through 1000ppm doped agarose (dark). Following irradiation, the plates were placed in the incubator at 37 C 5% C02. Once a day for 5 days, fluorescent images were taken using the Zeiss Lumar V12 Stereoscope with an exposure time of 1500ms and a Rhodamine filter.

The images from this experiment were challenging to analyze due to high background and clumping of colonies, so simulated images were created in order to verify the accuracy of the CellProfiler Pipeline. MATLAB was used to create 10 different images approximating the key features of images from the experiment. The approximated features include intensity, distribution, size distribution, variable background, colony overlap, and background noise. The colonies were created using circles of radii 3 to 8 pixels corresponding to radii of 26 μm to 69.4 μm with intensity 0.2 centered at random positions with a greater weight toward the center of the image. In this way, clumping was created similar to the experimental images. Next, a 2D gaussian was added to the image to mimic the background illumination we saw with a maximum value of 0.30 at the center. Finally, random noise was added with a mean of 0.01 and a standard deviation of 0.005. In order to approximate the intensity distribution of the experiment colonies, tapered edges were created such that the intensity decreased toward the edge of the colony. After running the image analysis, two more image sets were created with exaggerated tapering and no tapering of intensity toward the edges of the colony to test specifically the area measured by CellProfiler.

## 2.1 Experiment Images

Experimental images were acquired of tumor cell colonies growing on the brain slice model. These images were used to design simulated data that closely matched10000 4T1 mCherry murine mammary tumor cells were plated on 400 μm rat brain slices on top of transwell inserts within one corning 6 well plate. The cell media for 4T1 cells consisted of RPMI1640 (Gibco), 10% FBS (Tissue Culture Biologicals), Pen/Strep (Gibco), HEPES 10mM (Gibco), Sodium Pyruvate 1mM (Gibco), D-Glucose 0.25% (Sigma-Aldrich). The plates were incubated at 37 C, 5% CO2 and 90% humidity in between images. Images were taken every 24 hours for 5 days post radiation irradiation with Zeiss Lumar V12 Stereoscope with 17.6x magnification and +0.63mm focus. A Rhodamine filter with an exposure time of 2500ms, using the Zen Blue Pro software was used to take fluorescence images.

## 2.2 Simulated Images

MATLAB was used to create 10 different images approximating the key features of images from the experimental images. The approximated features include intensity, distribution, size distribution, variable background, colony overlap, and background noise. The colonies were created using circles of radii 3 to 8 pixels corresponding to radii of 26 μm to 69.4 μm with intensity 0.2 centered at random positions with a greater weight toward the center of the image. In this way, clumping was created similar to the experimental images. Next, a 2D gaussian was added to the image to mimic the

background illumination observed in real data with a maximum value of 0.30 at the center. Finally, random noise was added with a mean of 0.01 and a standard deviation of 0.005. In order to approximate the intensity distribution of the experiment colonies, tapered edges were created such that the intensity decreased toward the edge of the colony. After optimizing the pipeline for these simulated images, image sets were created with increasing colony count, increasing background, and increasing noise to further test the pipeline. In addition, image sets with exaggerated tapering and no tapering of intensity toward the edges of the colony to test specifically the area measured by CellProfiler. Below in Figure 4, images from the experiment on days 3,4,5 are compared to the simulated images approximating them.

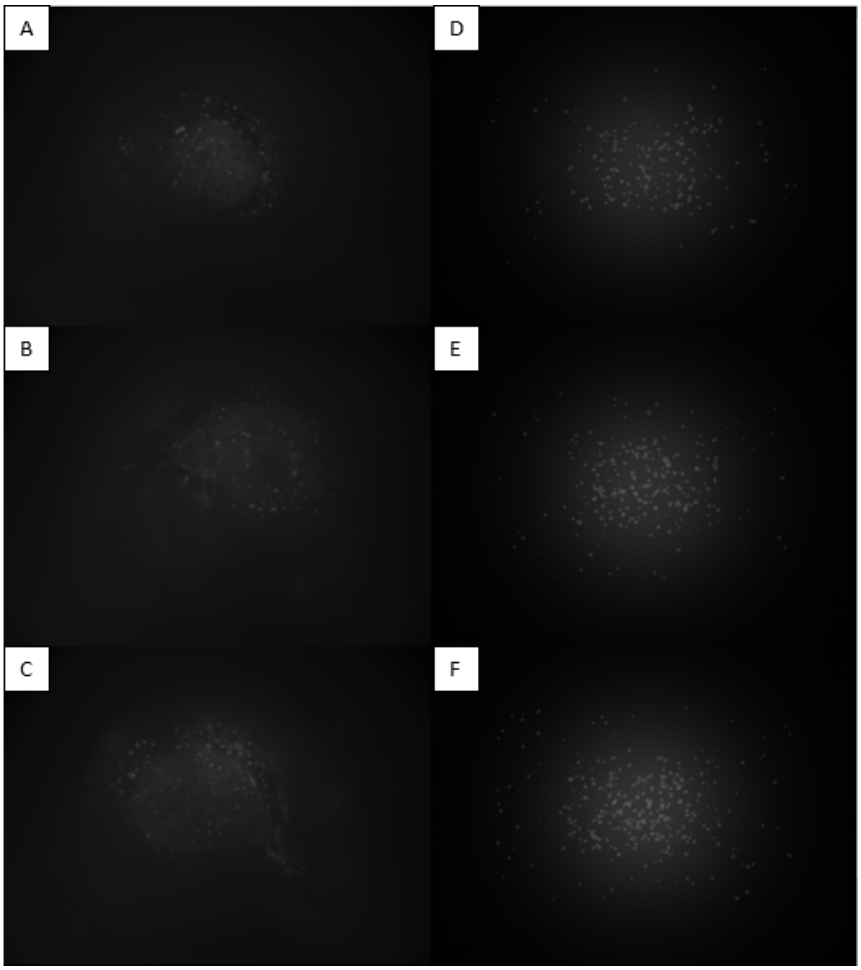


**Figure 4: A,B,C) Images taken with Zeiss Lumar V12 Stereoscope of 4T1 cells from days 3,4,5. D,E,F) Simulated images approximating images from days 3,4,5. Approximated features include colony intensity, distribution, size distribution, variable background, colony overlap, and background noise.**

## *2.3 CellProfiler Analysis*

A CellProfiler pipeline was optimized to analyze the simulated MATLAB images. The outputs from this pipeline are count, area, and integrated intensity of colonies. Each of these metrics had a known ground truth through MATLAB and the CellProfiler measurements were compared to these values. Below is a schematic for the pipeline.

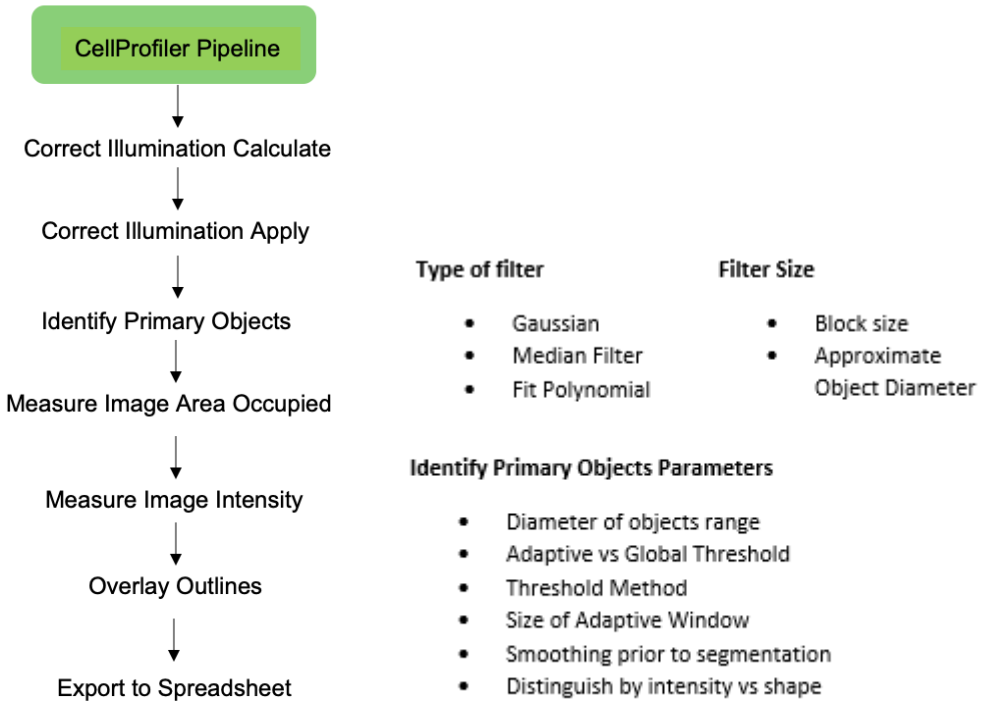


**Figure 5: CellProfiler Pipeline Schematic. A median filter with a block size of 20 pixels was used to create the background image that was subtracted. The diameter range for colonies was 3 to 20 pixels corresponding to radii of 26 μm to 173.3 μm. The adaptive window used was 15 pixels using an otsu threshold method. Objects de-clumped using intensity.**

Correct illumination Calculate and Apply were used to subtract background illumination using a median filter. Identify Primary objects segments the regions of interest using adjustable parameters (Figure 5). Changes were made to diameters allowed for objects, minima and maxima intensities, and the smoothing scale prior to segmentation. An adaptive window was also used in order to allow different cutoff intensities in different regions of the image. Each of these parameters was adjusted until the pipeline was accurately segmenting the colonies within the image.

## *2.4 Integrated Intensity Analysis*

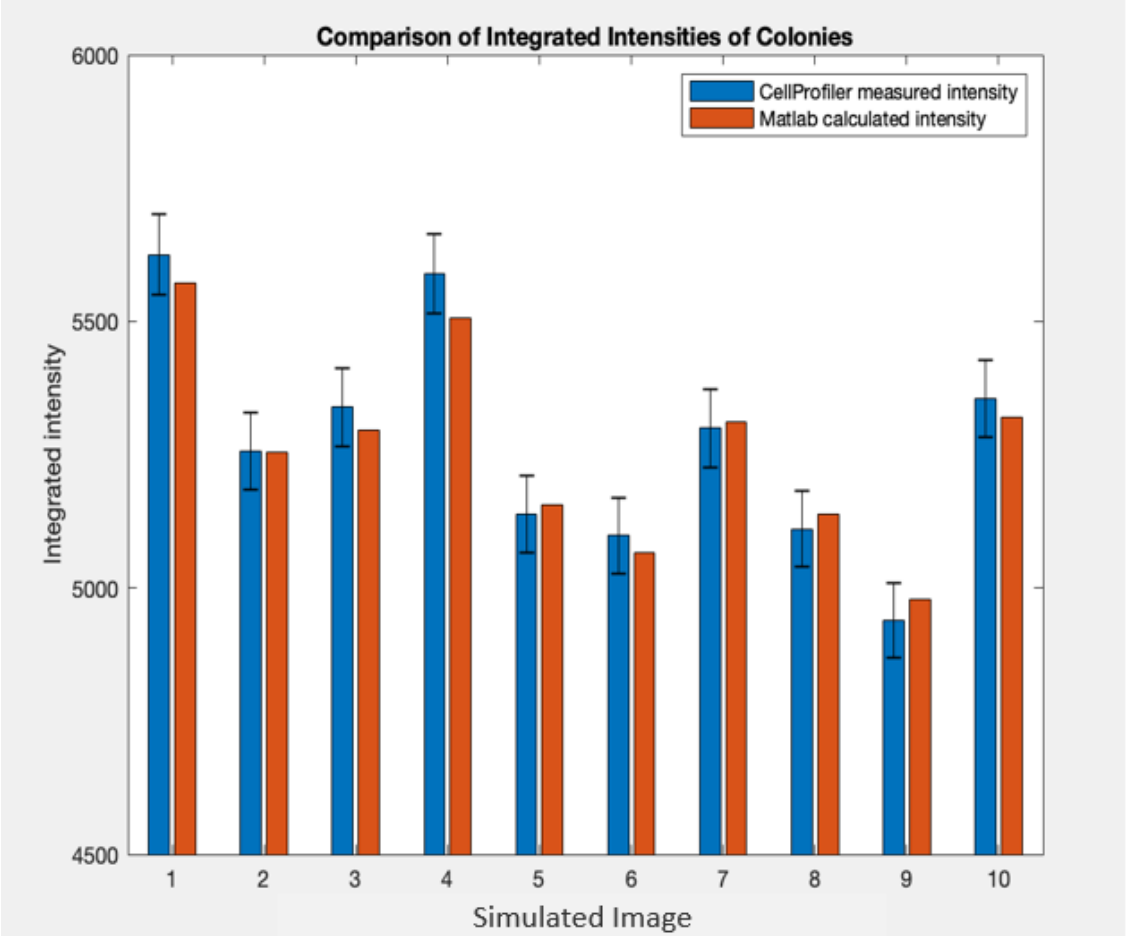


**Figure 6: Integrated intensities of the 10 simulated images approximating days 4-5 from the experiment - CellProfiler measured intensity (blue) and MATLAB calculated intensity (red). Error range in measured intensity for CellProfiler calculated by changing inputs of pipeline to reasonable minima and maxima. The CellProfiler pipeline measured integrated intensity of the 10 simulated images with an accuracy of 99.23% ± 0.75%.**

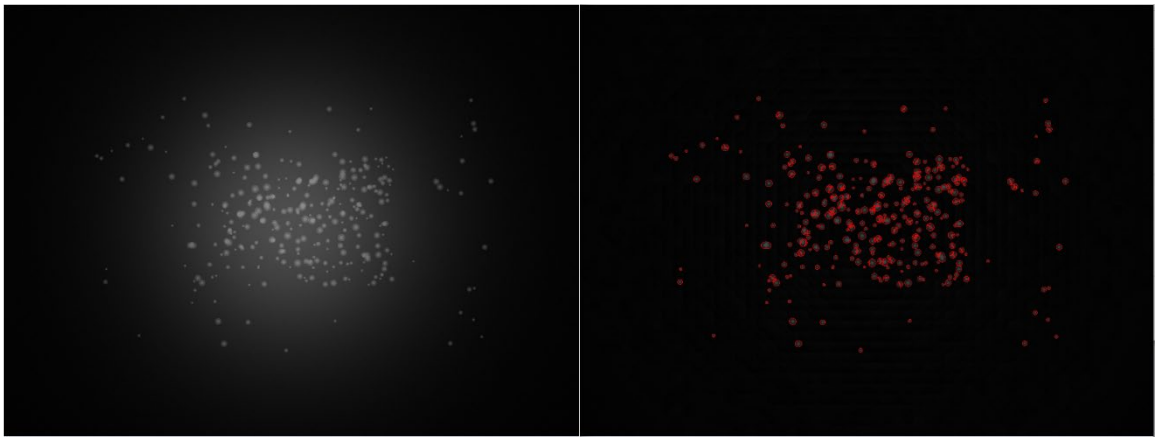

**Figure 7: (Left) Simulated image with approximating original image set. (Right) Segmented colonies after background subtraction with CellProfiler pipeline. Close agreement can be seen in the overlaid image of segmentation.**

The optimized CellProfiler pipeline accurately measured integrated intensity of the colonies within the simulated images (99.23% ± 0.75%) (Figure 6). Segmented area displayed as outlines depicts the accurate segmentation (Figure 7). This result gave confidence that the same pipeline could be used to measure integrated intensity in the 4T1 mCherry images. In order to further test the pipeline, measurements of integrated intensity were made on simulated images with increasing colony count, background intensity, and noise intensity.

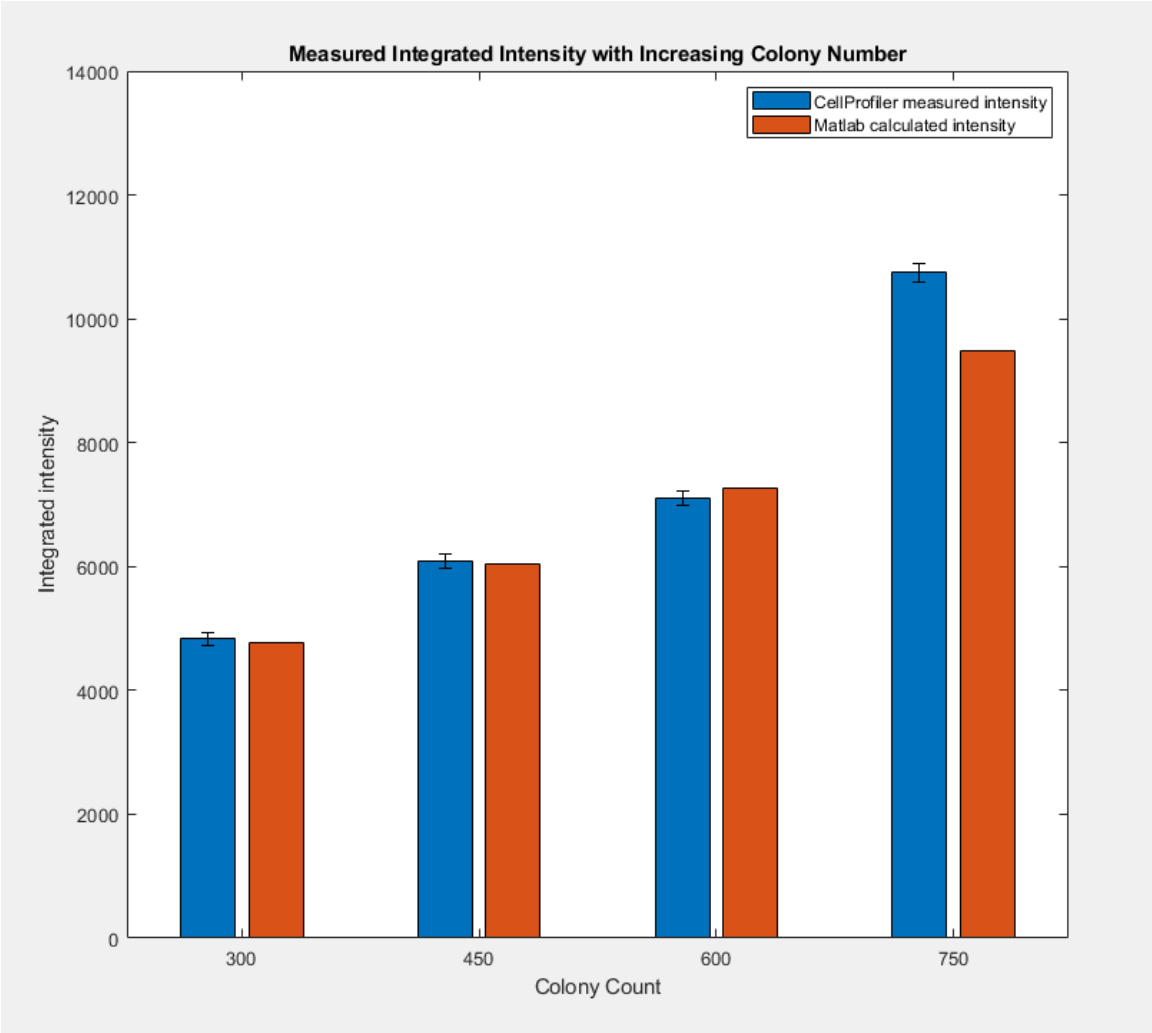


**Figure 8: With increasing colony count, the CellProfiler pipeline accurately measured integrated intensity for 300, 450, 600 colonies (98.68% ± 2.05%, 100.9% ± 1.81%, 97.6% ± 1.98%). For the experimental images, there were no more than 500 colonies. At the maximum colony count of 750 colonies, the pipeline overestimated intensity at 113.46% ± 1.85%.**

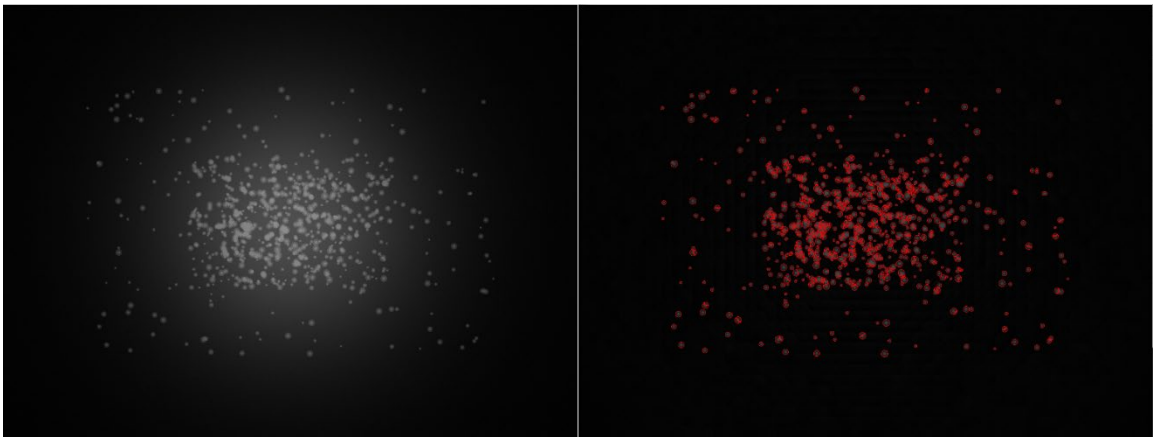

**Figure 9: (Left) Simulated image with 750 colonies. (Right) Segmented colonies after background subtraction with CellProfiler pipeline. Significant cell clumping observed yielding larger area colonies and challenges with segmentation.**

The CellProfiler pipeline was accurate in measuring integrated intensity up until 600 colonies per image (Figure 8). Given that the pipeline was optimized for images with 300 colonies, it was expected that when the colony count increases substantially that there are difficulties in segmentation. After several tests of 750 colonies, the measured integrated intensity was still greater than the ground truth. This was likely due to issues with background subtraction with increased clumping (Figure 9).

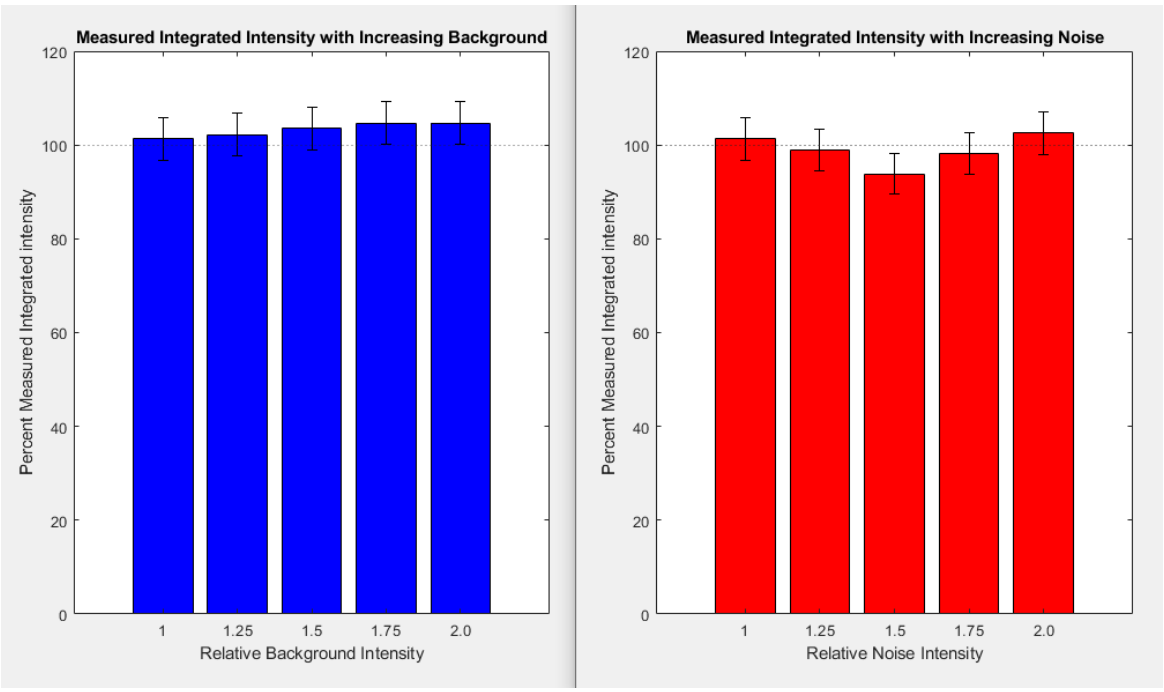


**Figure 10: (Left) Increasing background intensity increased CellProfiler measured intensity relative to ground truth. (Right) Increasing noise intensity did not have a systematic effect on CellProfiler measured intensity relative to ground truth.**

The measured integrated intensity increased as the background intensity increased; however, the values were still within 4.2% of ground truth (Figure 10 left). This increase is because the background cannot be entirely subtracted from the segmented areas. Surprisingly, the level of noise did not have a systematic effect on measured intensity (Figure 10 right).

Integrated intensity is the preferred metric for this experiment because it is proportional to the number of viable cells expressing the mCherry protein. Area is a less useful metric due to the inability to accurately measure clumped colonies. Although this is the

case, to further test the pipeline, an analysis was done using area to test the limitations of the pipeline.

## 2.5 Area Analysis

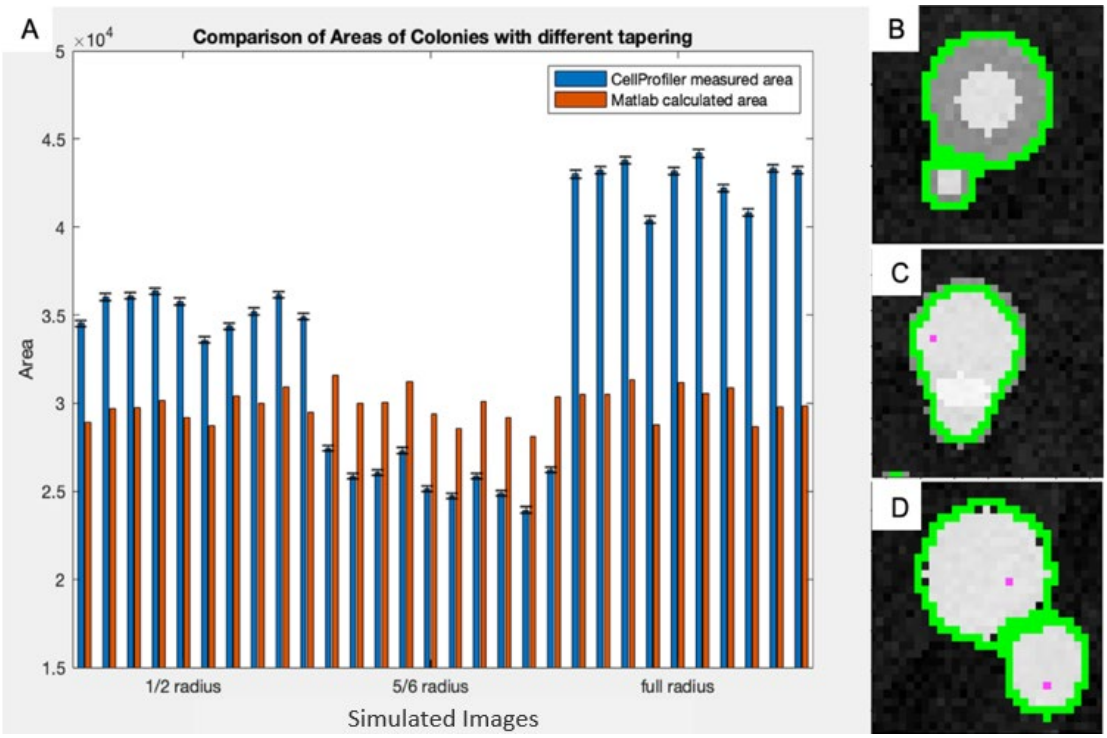


**Figure 11: Three sets of 10 simulated images each with different tapered edges. A) Bar graphs of area for exaggerated taper, image approximate and no taper. B) CellProfiler edge as determined in exaggerated taper overestimated area by 18.79% ± 4.82%. C) CellProfiler edge as determined in the image approximate underestimated area by 13.79% ± 1.09% D) CellProfiler edge as determined in no taper overestimated area by 41.52% ± 4.28%**

Total area analysis of area of colonies of the 10 simulated images that approximated day 4-5 from the experiment found that there was consistently a 13.79% ± 1.09% underestimation (Figure 11). Given this error, two more sample image sets were tested with exaggerated and no taper toward the edge of the colonies to see if there was any improvement based on colony intensity distribution. The pipeline overestimated

the area for the two by 18.79% ± 4.82% and 41.52% ± 4.28% respectively. Surprisingly, although the pipeline accurately measured integrated intensity, it struggled to accurately measure area.

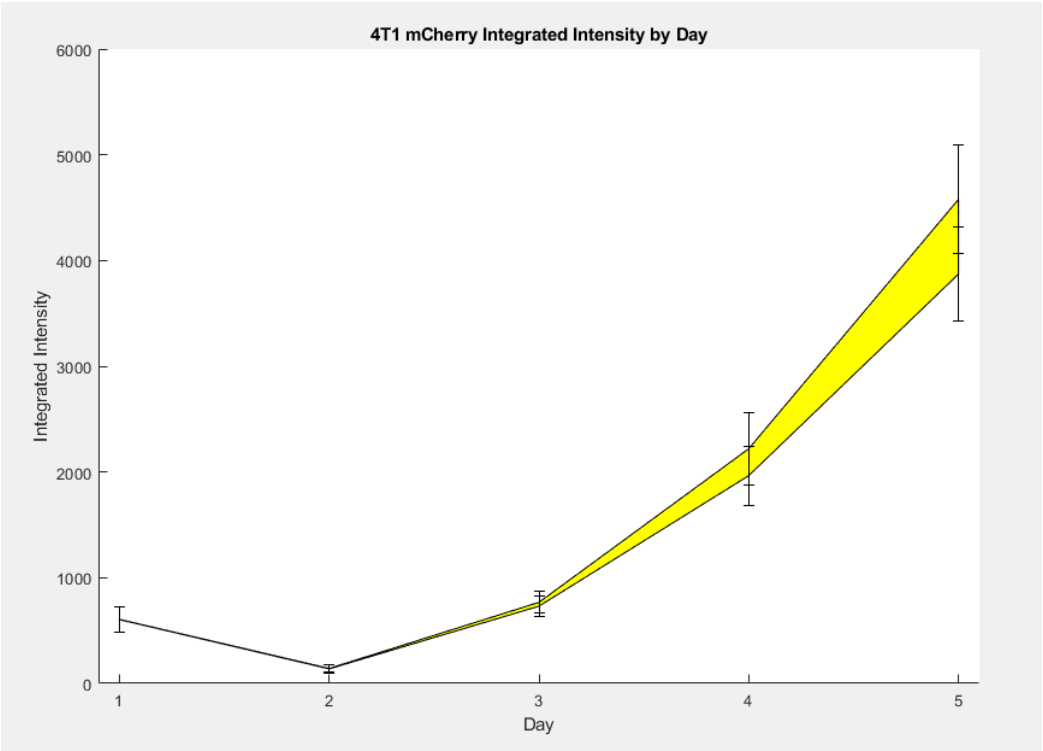


**Figure 12: Graph of 4T1 mCherry integrated intensity by day. Yellow area representative of range of outputs with reasonable minima and maxima in CellProfiler pipeline output. Error bars displayed as one standard deviation between 6 wells.**

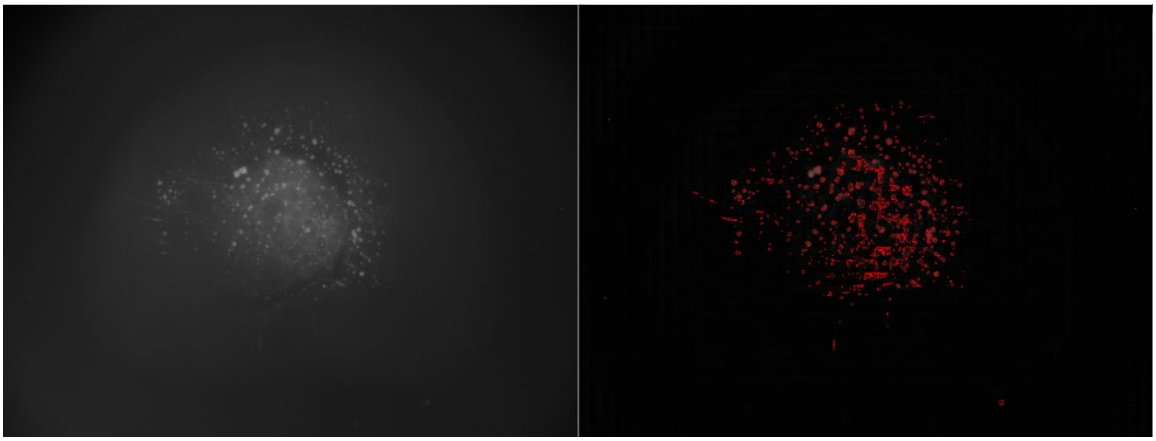

**Figure 13: (Left) Day 4 image of 4T1 colonies from original experiment. (Right) Segmented colonies after background subtraction with CellProfiler pipeline. Accurate segmentation appreciable with subtracted background.**

This pipeline found an approximate doubling of integrated intensity each day within the segmented 4T1 cell images after day 2 (Figure 12). The decrease from day 1 to day 2 was most likely attributable to plating efficiency. The doubling time of 4T1 cells is 13.6 ± 1.5 hours and this yields an increase of a factor of 3.4 daily. The increase in integrated intensity was closer to this value starting at day 2 when there were fewer cells. It is hypothesized that as clumping of cells increased with time, the intensity of mCherry signal is no longer linearly proportional to the number of viable cells. CellProfiler accurately segmented the colonies within the images (Figure 13).

## *2.6 Image analysis Conclusions*

After optimization of the CellProfiler pipeline, it accurately measured integrated intensity of the colonies within the simulated images (99.23% ± 0.75%). This same pipeline did a good job of measuring the integrated intensity for simulated images with increasing colony count until 600. Past this point the clumping was substantial and

prevented accurate background subtraction. The pipeline did a reasonable job of subtracting the background in images with increasing background, but as expected, the relative measured value for integrated intensity increased. Surprisingly, increased noise did not have a systematic effect on the measured integrated intensity value. The fact that the pipeline was less accurate with increases in any of the features tested illustrates the point that it is important to tailor the inputs of the software to the data set. The experiment image set had some variability in these parameters, but not to the extremes that were tested.

This optimized pipeline was used to measure the images from the 4T1 experiment images. The increase in signal following day 2 of the experiment was close to what was hypothesized given the doubling time of 4T1 cells. As clumping increased in subsequent days, cells behind another did not contribute as much to integrated intensity, and this is plausible explanation for why the rate of increase decreased with subsequent days. The decrease in signal from day 1 to day 2 can be explained by cell plating efficiency.

CellProfiler was also found to have difficulty in accurately measuring the area of the simulated images. The reason CellProfiler was consistently under or over approximating the area of colonies was due to the built-in algorithm for detecting an edge. This error is most pronounced in the images with colonies with no taper in intensity toward the edges, indicating sharp edges do not yield accurate area of colony

measurements with CellProfiler. Although there was error in the area measurements, the error was consistent, and the area metric could still be used for comparison between images.

It is important to have a repeatable accurate analysis of image metrics. Using simulated images to confirm the validity of the analysis tool was helpful for this experiment. A similar technique may be prudent for experiments with images containing new features.

## 3. Preparatory Work

# Preparatory Work

### 3.1 Wavelength and energy fluence to activate psoralen

- Experiments with 254nm light (UVB) had significant cytotoxicity from the UVB alone and no significant difference between ± Psoralen arms.
- Switched from 254 nm UVB to 365 nm UVA and found significant increase in cytotoxicity at 0.5,1 J/cm$^2$ UVA with psoralen

### 3.2 Optimal psoralen loading technique

- Different loading techniques had been tested altering psoralen concentration and time of co-incubation.
- Found significant effect with 1 μM psoralen co-incubated for 1 hour prior to plating.

### 3.3 What is the more potent psoralen?

- Comparison of AMT (4'-Aminomethyltrioxalen) to 8-MOP (8-Methoxypsoralen) revealed AMT as a more potent derivative.
- For 1J/cm$^2$ the AMT and 8-MOP trials had 98.3%±0.3% and 93.1%±0.5% cell death, respectively.

### 3.4 Validating pipeline on Cell titrations

- Tested plates with increasing cell number plated to analyze mCherry signal output from CellProfiler.
- The growth in fluorescent signal was consistent and different cell titration platings were differentiable by signal.
- 20k outlier likely due to plating error

**Figure 14: Summary of preparatory work done to determine the best protocol for the RECA experiment.**

This thesis presents a highly sophisticated main experiment involving many critical steps. Failure at any individual step (to name a few: insufficient psoralen loading

in cells, inadequate initial tumor cell plating, inadvertent light exposure, or inadequate imaging parameters) could compromise the entire experiment. For this reason, much preparatory work was performed prior to the main experiment, in order to verify that each step was performed correctly (Figure 14). Many experiments paved the way for the present experiment evaluated in this work. Improving the image analysis technique using simulated images was a large focus. In addition, several techniques were refined including psoralen loading concentration and time, type of psoralen, number of plated 4T1 cells, exposure time on microscope.

## *3.1 Wavelength and energy fluence to activate psoralen*

Initially, experiments were conducted using a Stratalinker 1800 to deliver 254nm light at different determine the optimal energy fluence and to test different psoralen loading techniques (discussed later). It was found that there was significant cell death after 48 hours at $0.5 J/cm^2$ of 254 nm light in both the psoralen treated cells and control group. Additionally, there was not a significant difference between with and without psoralen groups. After switching to 365nm light for activation we found a significant difference between psoralen treated cells and control group at several different energy fluences. Further preparatory work was conducted using 365nm light.

## *3.2 Optimal psoralen loading technique*

Experiments were conducted testing the optimal concentration of psoralen, loading technique, and type of psoralen. Extensive testing into the relative efficacy of different psoralens was conducted by Buhimschi *et al.* 2020[5]. In this work, the psoralens were incubated at 1 μM for 1 hour with the B16 murine melanoma cells and tested for cytotoxicity after activation with 1 J / $cm^2$ 365 nm light. The fact that this work had chosen to use 365 nm light as well to activate psoralen was reassuring. Prior RECA work had used psoralen concentrations of 10-100 μM co-incubating for 2 hours with the cells[15]. This concentration was used to approximate concentrations used in PUVA therapy. For this work, it was decided to use the lower 1 μM concentration for 1 hour considering the efficacy seen within the Buhimschi paper with this method.

### *3.3 What is the more potent psoralen?*

Two of the psoralens tested in the Buhimschi et al. paper were 8-MOP (8-methoxypsoralen) and AMT (4'aminomethyltrioxsalen). Cell survivals of 31.3% ± 3.7% and 0.43 ± 0.22% were observed using 8-MOP and AMT respectively. Given the

cytotoxicity levels with this psoralen loading technique, and the increased potency of AMT relative to 8-MOP, we attempted to replicate the findings in this study.

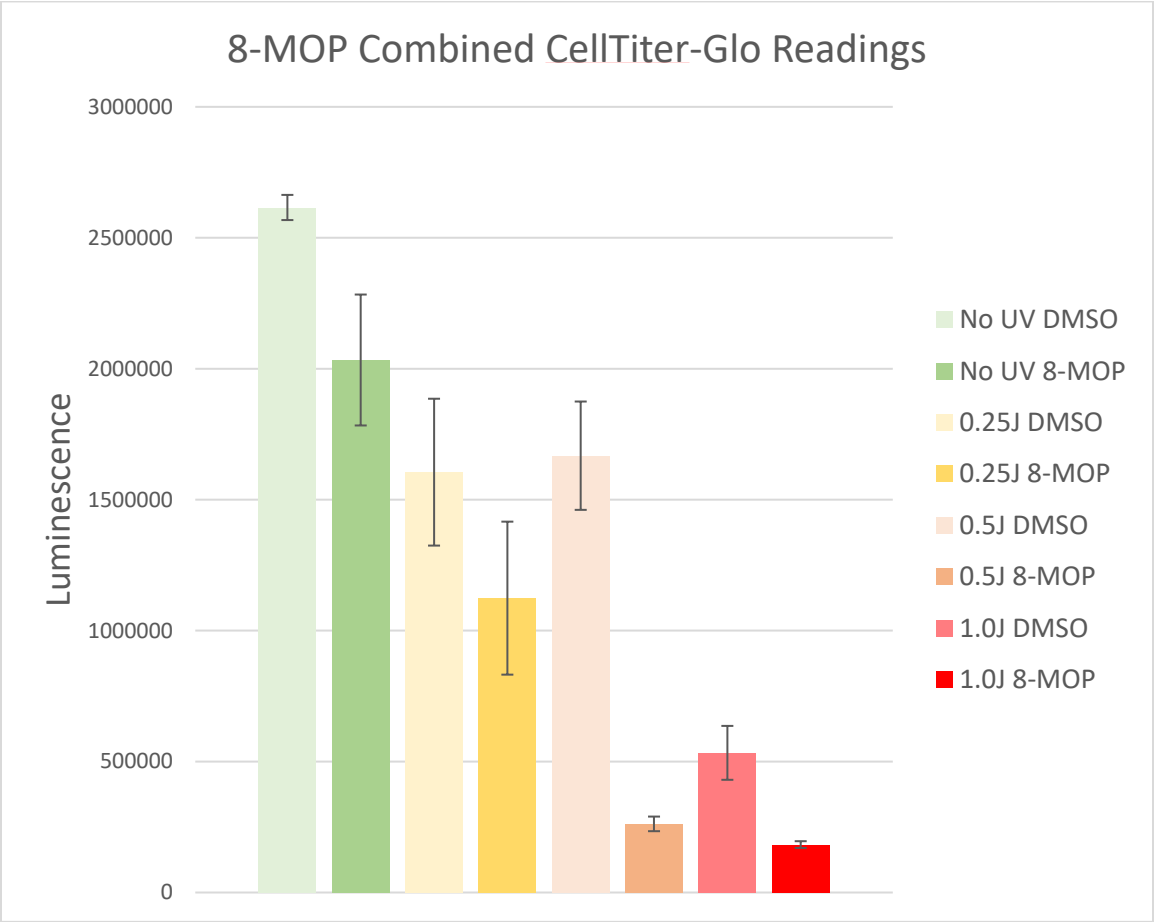

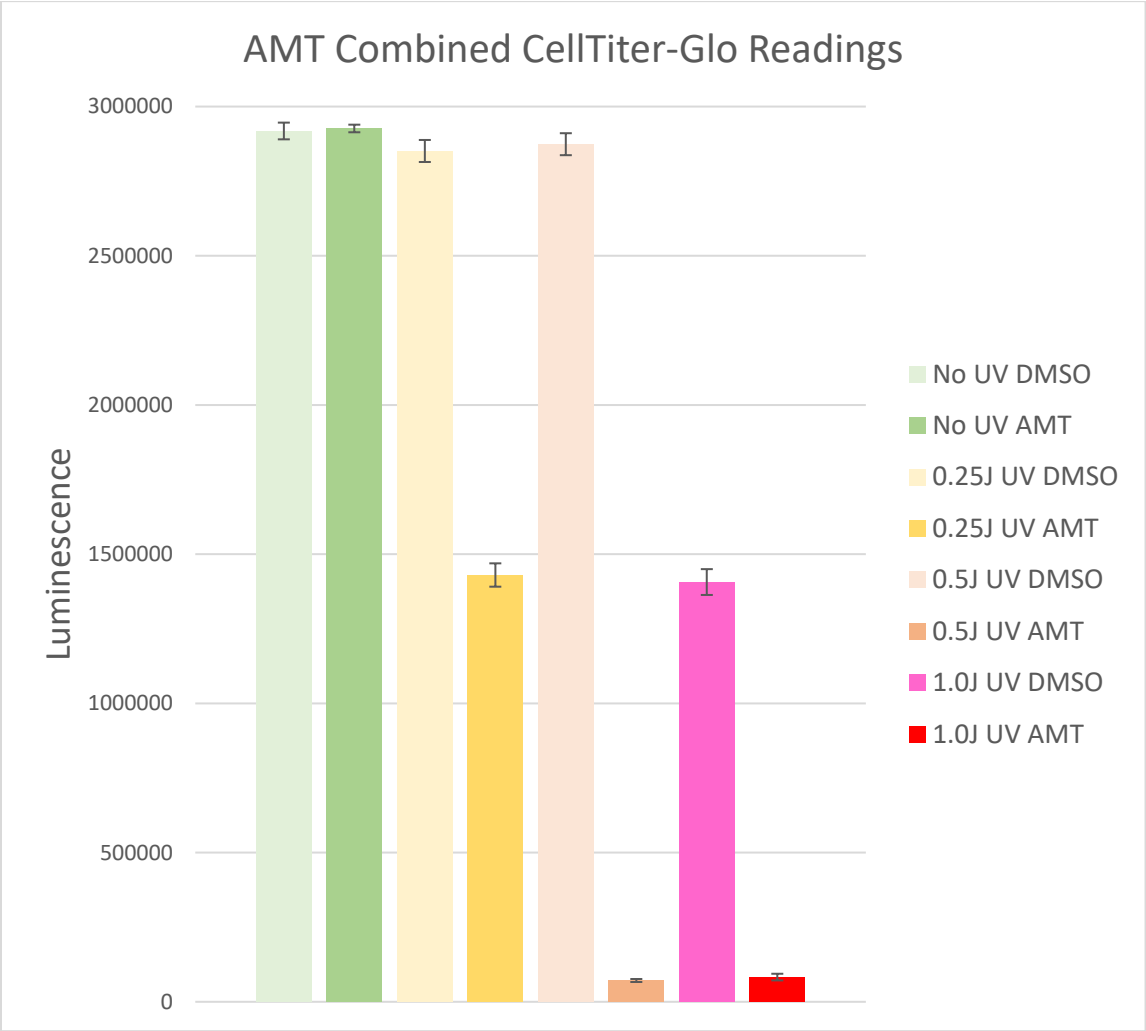


**Figure 15: Graphs of 4T1 mCherry Fluc cells exposed to 1 μM of 8-MOP (top) and AMT (bottom). The combined values from the CellTiter-Glo assays were used to determine the relative viability at each energy fluence of 365 nm light. A significant increase in cytotoxicity was observed for AMT relative to 8-MOP at the 0.5 J/cm² and 1J/cm² levels. Dose rate**

We were able to replicate the findings in the paper with AMT having significantly higher cytotoxicity than 8-MOP and verifying that our psoralen loading technique was appropriate. For 1J/cm² the AMT and 8-MOP trials had 98.3%±0.3% and 93.1%±0.5% cell death, respectively (Figure 16). We decided to use this same psoralen

loading technique of 1 μM AMT co-incubated for 1 hour prior to plating in our rat brain slice in-vitro experiment.

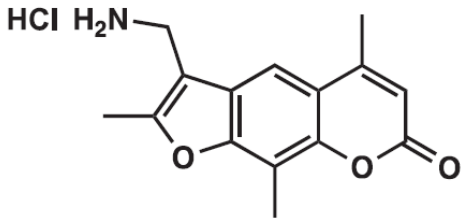


**Figure 16: 4′-Aminomethyl-4,5′,8-trimethylpsoralen (AMT) molecule. Addition of the 4′ methyl group found to increase potency for many psoralen derivatives[5].**

## *3.4 Validating Pipeline on Cell Titrations*

In addition to using the simulated images to verify the pipeline, the pipeline was used on titrated numbers of 4T1 cells plated on rat brain slices and incubated over 3 days. Six wells were used with 10k, 20k, 30k, 40k, 50k cells per well plated on 400μm rat brain slices. The wells were imaged using the Zeiss Lumar microscope each day for three days at 2000 ms exposure. These images were analyzed for integrated intensity on the same optimized pipeline.

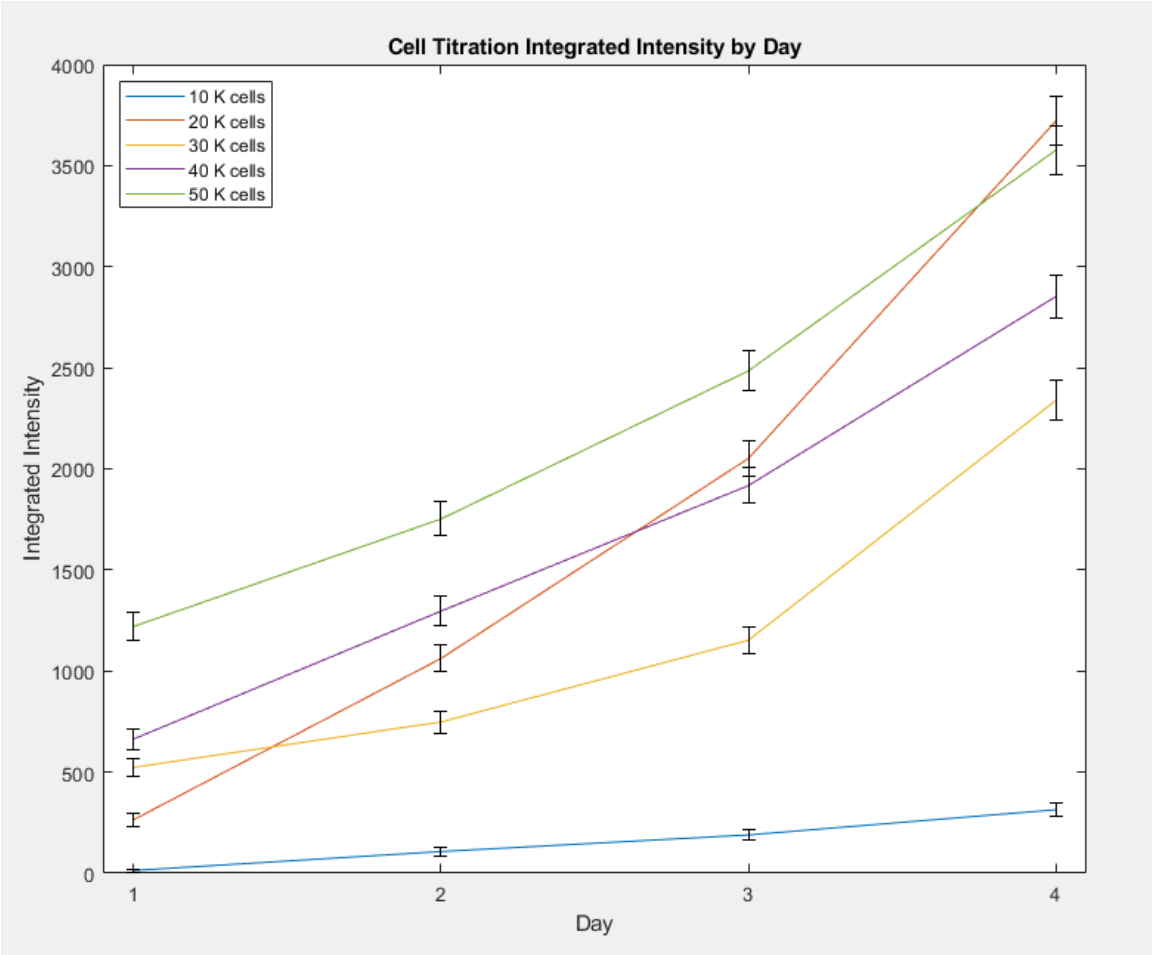


**Figure 17: Integrated intensity as output from CellProfiler by day for each cell titration. Error bars displayed as reasonable minima and maxima from CellProfiler output. Steady increase in growth for each titration along with consistent difference between titrations except for 20 K cells. The 20k well had a ring of what appeared to be colonies around the outside of the slice adding to the overall signal. It was hypothesized that the cells were accidentally plated in such a way that the cells flowed to the outside allowing more room for the colonies to grow.**

The experiment confirmed that the pipeline was able to distinguish between the different cell titrations, even on subsequent days (Figure 15). Additionally, the growth in signal for the plates was consistent except for 20k having increased growth and 10k

having decreased growth. The cause for the increased signal from the 20k images was the apparent ring of colonies around the edges of the brain slice adding to the signal. These are likely cells accidentally displaced during plating.

# 4. Methods

800mL of deionized water was mixed with 4g of agarose and boiled before pouring into a 19.5 x 19.5 cm flat bottom backing pan to yield a final agarose slab with dimensions 19.5 x 19.5 x 2 cm. This agarose slab was created to place underneath the cell plate such that the total depth will be 3cm at the level of the brain slice.

Six 12-well agarose plates with 1cm of agarose in each well were created using the same technique. 400 μm thick coronal rat brain slices were placed on top of each 1cm agarose within the well. 4T1 cells expressing both mCherry-flourescent and firefly luciferase-luminescent reporter proteins were used. 2.9 million 4T1 cells were suspended in two microcentrifuge tubes containing 432 μL of culture media augmented with 4.356 μL of DMSO or 100 μM AMT stock. Next, the tubes were and incubated for 60 minutes at 37 C 5% CO2 for 60min. After incubation, the cells in the tubes were resuspended by pipetting up and down. 3 μL aliquots containing 20,000 cells with DMSO were plated on each rat brain slice hemisphere within 3 plates. 3 μL aliquots containing 20,000 cells and AMT were plated on each rat brain slice hemisphere within the 3 remaining plates. The cells were plated with a yellow light with no UV emission

and no other lights. The plates were immediately covered in tin foil and placed into Styrofoam containers at room temperature following plating to eliminate incident light activation.

The six 12-well plates were each assigned to a different arm of the experiment. The six arms were MV DMSO, MV AMT, kV DMSO, kV AMT, No irradiation DMSO, No irradiation AMT. The plates receiving MV irradiation used the following schematic.

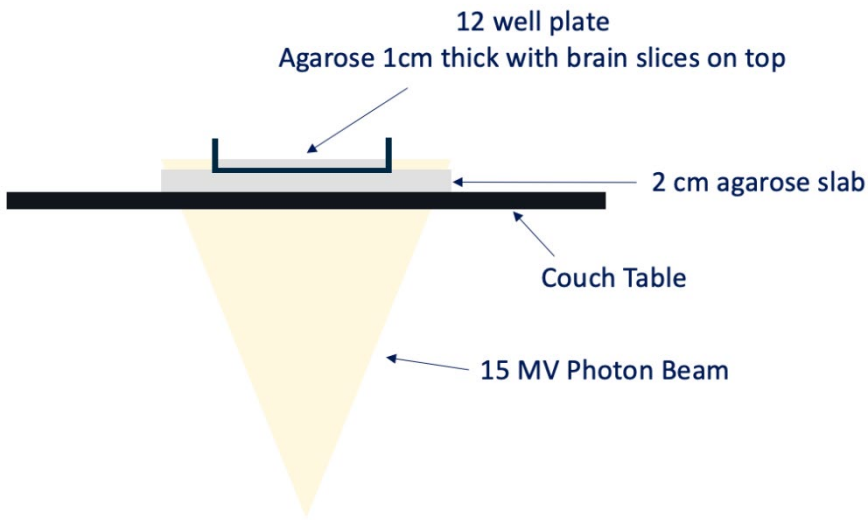


**Figure 18: Schematic of MV irradiation setup.**

A 19.5x19.5x2cm agarose slab placed below the 12 well plates to make the total depth of 3cm of agarose at the rat brain slice. Agarose was used over solid water due to the increased Cherenkov generation as found in Jain *et al.* 2019[16]. The reason for this thickness was to be at dmax for the 15 MV beam – a region where changes in depth have a small impact on total dose. A PA 15 MV 20x20cm field beam was delivered at 400 MU.

Following irradiation, the plates were re-wrapped in foil and placed back in the Styrofoam container to be transported to the incubator.

The plates receiving kV irradiation were treated with an XRAD 160 irradiator at 160 keV to 4 Gy and were then re-wrapped in foil and placed back in the Styrofoam container to be transported to the incubator.

The plates receiving no irradiation were kept in the Styrofoam box until being placed in the incubator at the same time as the plates from the other arms.

The plates were incubated at 37 C 5% CO2 for 5 days. Every 24 hours for 5 days the plates were imaged with the Lumar Zeiss microscope at 1500 ms exposure.
A CellProfiler pipeline was modified to accurately segment the colonies within these images. Modifications in block size for median filter, average colony diameter, smoothing filter, and adaptive block size were made until segmentation was optimal. This optimized CellProfiler pipeline measured the integrated intensity from colonies within the rhodamine filtered images.

After the day 5 images were taken, a firefly luciferase assay was done to quantify the number of living 4T1 cells. 150 μg/mL of Luminol was dissolved in PBS. 500 μL of this solution was placed in each well directly on top of the brain slices. Plates were re-wrapped in foil and incubated for 10 minutes at room temperature. Luminescence readings were taken using SpectraMax dual Luciferace assay. The settings were 12 well

standard opaque, 20mm height, 3mm depth, integration 140ms, read height 1.00mm.

The well scan settings were fill pattern, 13 density, 1.44mm spacing at 137 total points.

# 5. Results

## *5.1 RECA 4T1 mCherry image analysis*

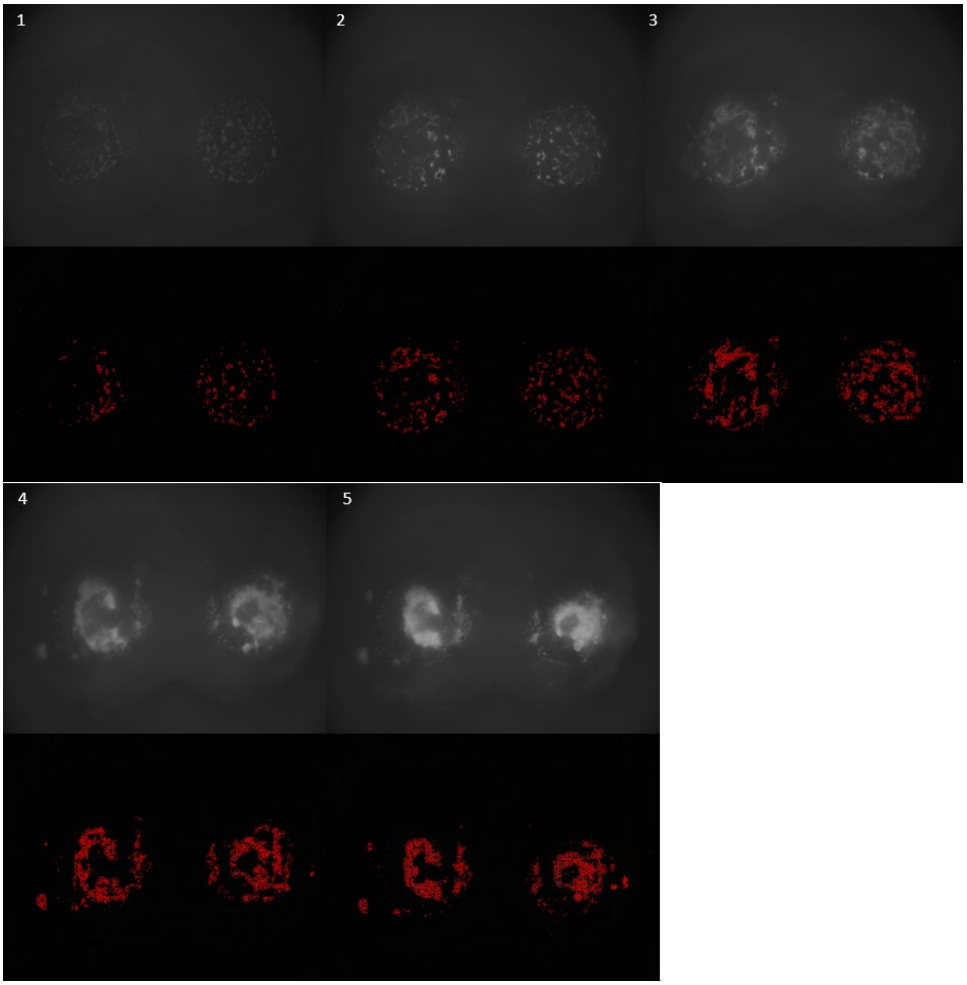


**Figure 19: (Top row) Grayscale image of mCherry filtered signal using Zeiss Lumar Microscope from AMT Dark well 6 for 5 days. (Bottom row) Segmented colonies after background subtraction using CellProfiler pipeline.**

The optimized CellProfiler pipeline accurately subtracted the background signal and segmented the colonies (Figure 19). By day 5 there was significant background and

cell clumping making it difficult to distinguish a colony from the background signal. Despite this challenge, the final segmented images do not appear to be significantly different than what would have been done by hand – the gold standard.

Another challenge with this image data set was that there were punctuated areas of what appeared to be holes with surrounding luminescence specifically in the AMT MV arm. This luminescence was challenging to subtract completely while still accurately segmenting, and this added to the overall signal from this arm. It was hypothesized that the cause of the punctuated areas had to do with the part of the rat brain the slice originated from. Given that the slices were sequentially plated, this hypothesis made sense given we only observed it in a subset of specifically the AMT MV arm.

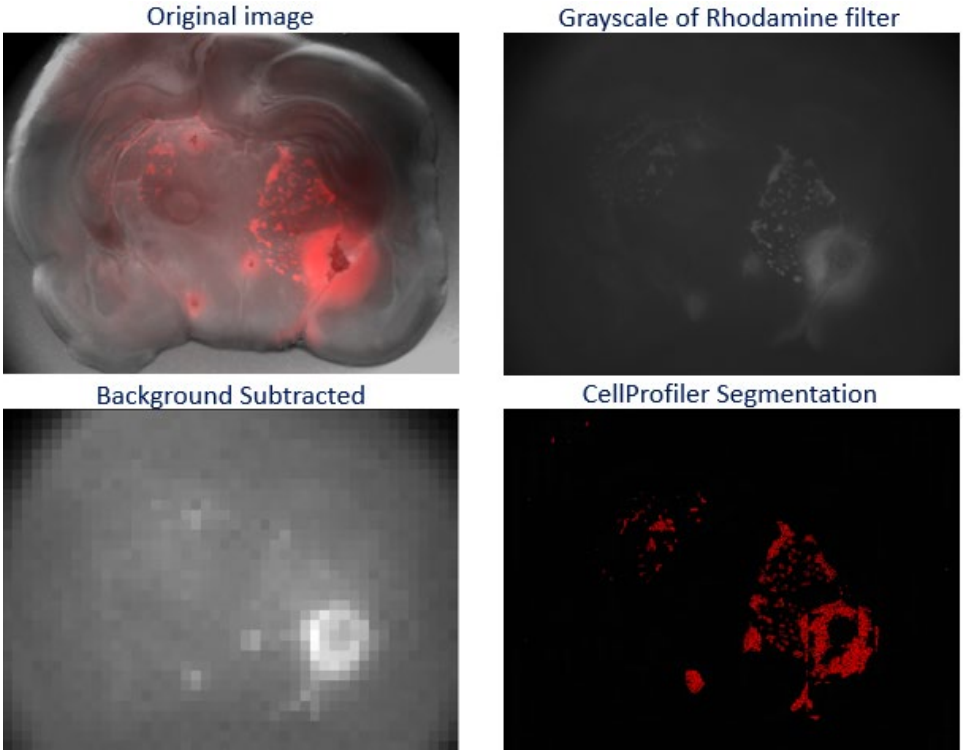


**Figure 20: AMT MV Well 9 day 1 original microscope image (Top left), Grayscale of Rhodamine filter (Top right), CellProfiler background subtracted (Bottom Left), and segmentation by CellProfiler after subtracting background (Bottom right).**

Background subtraction did eliminate much of the illumination from the punctuated spots within this arm (seen in bottom right of image in Figure 20); however, these areas still contributed to total integrated intensity. As the size of the median filter used for background subtraction decreases, the more accurate the background subtraction becomes. However, once the median filter used is small enough, it starts to subtract larger colonies. This is an example of a case in which it is important to finely tune the image analysis software, in this case CellProfiler, to best measure the data set. Integrated intensity was measured for each well and day as a metric that is directly

proportional to the number of viable cells. Below is a normalized graph of integrated intensity relative to day 1 for each plate.

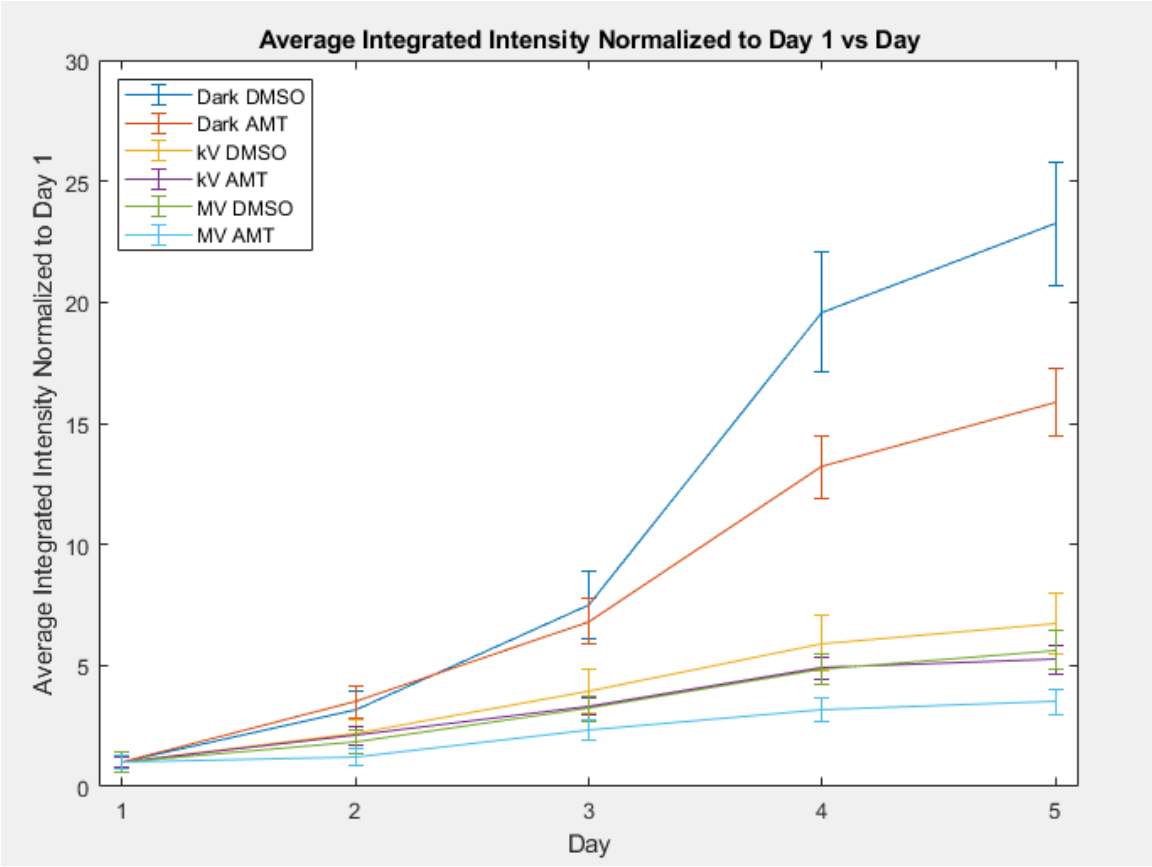


**Figure 21: Average integrated intensity normalized to day 1 for each arm of the experiment. A significant decrease in proliferation is observable for each AMT arm with the most significant being the decrease in proliferation from MV DMSO (5.65±0.78-fold growth) to MV AMT (3.49±0.52-fold growth)**

With the normalized integrated intensity analysis, there was a significant decrease in proliferation from MV DMSO (5.65±0.78-fold growth) to MV AMT (3.49±-0.52-fold growth) (Figure 21). This result is suggestive that psoralen is being activated causing the decreased proliferation seen in AMT MV relative to DMSO MV. There was also a significant decrease in growth for all the irradiated plates relative to the dark

control plates. The kV control and kV AMT arms had a smaller decrease in proliferation when compared to their MV counterparts (6.73±1.24 and 5.26±0.59-fold growth respectively). Interestingly, there was also a significant decrease in proliferation for each AMT treated plate within a given radiation condition. This would suggest some sort of dark cytotoxicity with AMT that was not observed in previous in-vitro tests. Another possible explanation is activation of psoralen inadvertently during imaging with the microscope. The next analysis was the non-normalized integrated intensity by day.

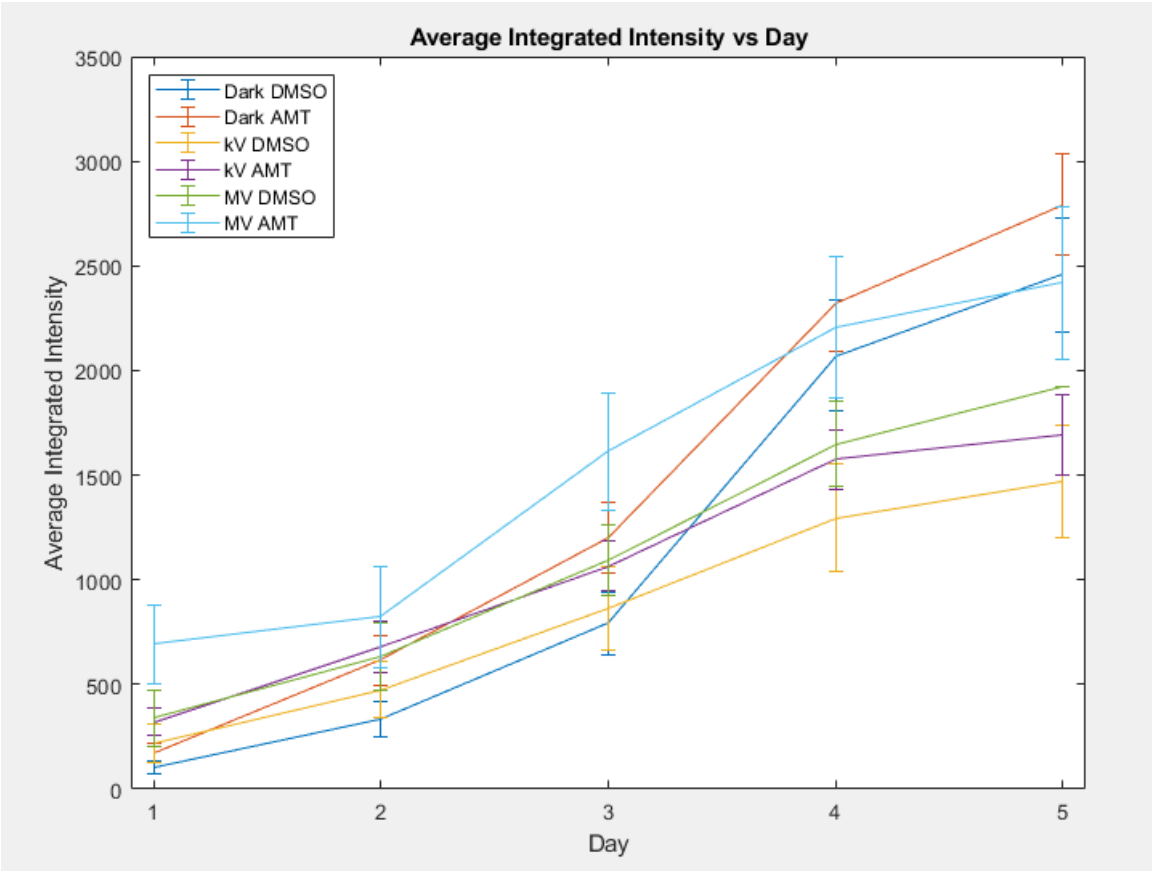


**Figure 22: Integrated intensity averaged over all 12 wells for each condition by day. Significantly larger MV AMT intensity on day 1 due to punctuated spots of increased signal. Day 5 intensity lower for each arm treated with radiation.**

There were significant day one differences between arms in integrated intensity with AMT MV being the largest with 693 $\sigma = 189$ while the other arms had between 100-350 (Figure 22). Part of this difference is explained by punctuated spots of increased signal in the AMT MV arm that were not able to be fully subtracted. Aside from this, the relative integrated intensity on day 5 corroborates what we expected with all irradiated arms having fewer viable cells. The signal within the non-irradiated plates increased at a rate consistent with the 13.6 ± 1.5 hr doubling time for 4T1 cells. The decrease in growth of signal from day 4 to 5 is likely attributable to clumping of cells causing a non-linear relationship between number of cells and signal. The values for integrated intensity on day 5 were used to compare relative to the firefly luciferace assay results below. Namely: Dark DMSO 2,457, Dark AMT 2,793, kV DMSO 1,471, kV AMT 1,693, MV DMSO 1,921, MV AMT 2,418

## *5.2 RECA luciferase assay*

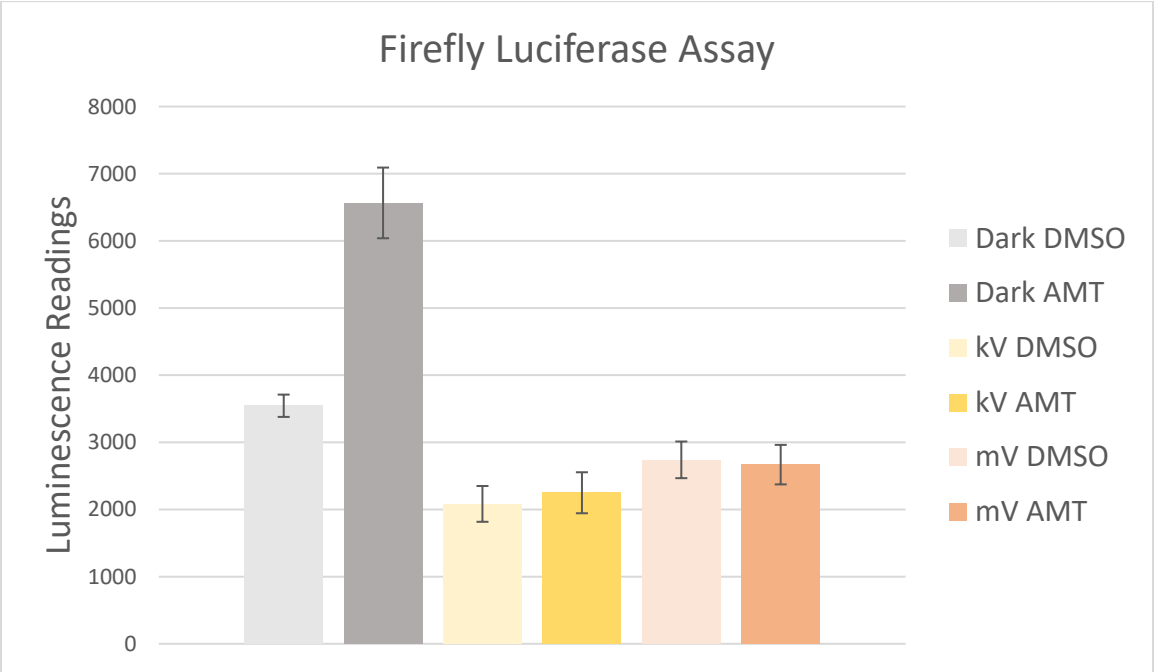


**Figure 23: Firefly luciferase assay day 5 readout. Significant decrease in viability for each radiated arm. Large inexplicable difference between both Dark arms.**

The luciferase assay results also showed a significant decrease in viable cells on day 5 for all irradiated arms (Figure 23). Additionally, the relative order of viability with Dark followed by MV followed by kV was found in both the luciferase assay and the integrated mCherry signal analysis. There is no present hypothesis for the difference between the dark DMSO and dark AMT luciferase assay results aside from variability in the assay itself.

# 6. Discussion

The preliminary results are consistent with psoralen activated in RECA treated cells and causing decreased proliferation for the MV arm (Figure 21). The growth observed in the Dark control arm was consistent with the 13.6±1.5 hour doubling time for 4T1 cells. There was also a significant decrease in proliferation for Dark AMT relative to Dark DMSO as well as kV AMT relative to kV DMSO. This was unexpected considering there was no significant cytotoxicity from non-activated psoralen in previous in-vitro experiments. This may be attributable to activation during imaging and will be investigated in the next experiment. Both the image analysis and luciferase assay showed decreasing cell proliferation from Dark to MV to kV arms. This agreement between the two tools to analyze cell viability on day 5 added to the confidence of the results.

There was minimal error in the dose from the kV irradiations as well as the MV irradiations. The X-RAD 160 used for the kV irradiations reports a 1% potential error in dose. The MV irradiation, given no backscattering surface with a 20x20 field at 400 MU the dose was within 3% of 4 Gy. Given the variability in both the luciferase assay and mCherry signal results, this potential error in dose is insignificant.

The punctuated spots of increased signal seen in the MV AMT arm was present in 7/12 of the wells. This was likely due to the portion of the rat brain used for that plate. The next experiment will use randomly selected rat brain slices to minimize the

chances that one arm will receive significantly more slices from one portion of the brain. The viability of the brain slice was assessed each day and found to be stable over the 5 days. Biological data is subject to many different uncontrollable variables and the experimental results warrant further investigation. A repeat of this experiment will help determine whether the effect observed is consistent.

# 7. Conclusions

The rat brain slice model is a distinct improvement over the 2D well plate for this experiment. The ability to generate Cherenkov light in tissue as well as allow the cells to grow in 3D better approximates an in-vivo experiment. Ultimately, an in-vivo experiment would help determine whether the effect seen in-vitro is reproducible or even exaggerated in a living animal with an intact immune system.

The results from the integrated intensity analysis were suggestive that psoralen was being activated and subsequently decreasing proliferation for the MV arm. This activation was likely the result of Cherenkov activation. Further work is needed to confirm and quantify the effect.

## References


1. Edelson, R., C. Berger, F. Gasparro, B. Jegasothy, P. Heald, B. Wintroub, E. Vonderheid, R. Knobler, K. Wolff, G. Plewig, G. McKiernan, I. Christiansen, M. Oster, H. Honigsmann, H. Wilford, E. Kokoschka, T. Rehle, M. Perez, G. Stingl and L. Laroche (1987) Treatment of cutaneous T-cell lymphoma by extracorporeal photochemotherapy. Preliminary results. N. Engl. J. Med. 316, 297–303.

2. Volc-Platzer, B., H. Honigsmann, W. Hinterberger and K. Wolff (1990) Photochemotherapy improves chronic cutaneous graft-versus-host disease. J. Am. Acad. Dermatol. 23, 220–228.

3. Melski, J. W., L. Tanenbaum, J. A. Parrish, T. B. Fitzpatrick and H.L. Bleich (1977) Oral methoxsalen photochemotherapy for the treatment of psoriasis: a cooperative clinical trial. *J. Invest. Dermatol.* 68, 328-335

4. dos Santos, D. J., & Eriksson, L. A. (2006). Permeability of psoralen derivatives in lipid membranes. *Biophysical journal*, *91*(7), 2464–2474. https://doi.org/10.1529/biophysj.105.077156

5. Buhimschi AD, Gooden DM, Jing H, et al. Psoralen Derivatives with Enhanced Potency. Photochemistry and Photobiology. 2020 Sep;96(5):1014-1031. DOI: 10.1111/php.13263.

6. Van Henegouwen, G., Wijn, E., Schoonderwoerd, S., & Dall'Acqua, F. (1989). A method for the determination of PUVA-induced in vivo irreversible binding of 8-methoxypsoralen (8-MOP) to epidermal lipids, proteins and DNA/RNA. Journal Of Photochemistry And Photobiology B: Biology, 3(4), 631-635. doi: 10.1016/1011-1344(89)80086-7

7. Oldham, M., Yoon, P., Fathi, Z., Beyer, W., Adamson, J., & Liu, L. et al. (2016). X-Ray Psoralen Activated Cancer Therapy (X-PACT). PLOS ONE, 11(9), e0162078. doi: 10.1371/journal.pone.0162078

8. Yoon, S., Tsvankin, V., Shrock, Z., Meng, B., Zhang, X., & Dewhirst, M. et al. (2018). Enhancing Radiation Therapy Through Cherenkov Light-Activated Phototherapy. International Journal Of Radiation Oncology*Biology*Physics, 100(3), 794-801. doi: 10.1016/j.ijrobp.2017.11.013

9. Čerenkov, P. (1937). Visible Radiation Produced by Electrons Moving in a Medium with Velocities Exceeding that of Light. Physical Review, 52(4), 378-379. doi: 10.1103/physrev.52.378

10. Sakaue, K., Brameld, M., Kuroda, R., Nishida, M., Taira, Y., Toida, T., Urakawa, J., Washio, M., & Yanagisawa, R. (2017). Investigation of the Coherent Cherenkov Radiation Using Tilted Electron Bunch.

11. Zhang R, Glaser AK, Gladstone DJ, Fox CJ, Pogue BW. Superficial dosimetry imaging based on Cerenkov emission for external beam radio- therapy with megavoltage x-ray beam. Med Phys. 2013;40:101914.

12. Hartl BA,Hirschberg H,Marcu L,Cherry SR.Activatingphotodynamic therapy in vitro with Cerenkov radiation generated from Yttrium-90. J Environ Pathol Toxicol Oncol. 2016;35:185–192.

13. GlaserAK,ZhangR,AndreozziJM,GladstoneDJ,PogueBW.Cheren- kov radiation fluence estimates in tissue for molecular imaging and ther- apy applications. Phys Med Biol. 2015;60:6701.

14. Shrock, Z., Oldham, M., & Adamson, J. (2016). SU-F-T-507: Modeling Cerenkov Emissions From Medical Linear Accelerators: A Monte Carlo Study. Medical Physics, 43(6Part21), 3580-3580. doi: 10.1118/1.4956692

15. Jain, S., Yoon, S., Zhang, X., Adamson, J., Floyd, S., & Oldham, M. (2019). Evaluation of UVA emission from x-ray megavoltage-irradiated tissues and phantoms. *Physics In Medicine & Biology*, *64*(22), 225017. doi: 10.1088/1361-6560/ab4333

16. Liu, X., Chen, X., Bowsher, J., Oldham, M., (2020) A New Method to Investigate RECA Therapeutic Effect. Duke Kunshan and Duke University

17. C. Humpel Organotypic brain slice cultures: a review Neuroscience, 305 (2015), pp. 86-98, 10.1016/j.neuroscience.2015.07.086

18. Clarke ML, Burton RL, Hill AN, Litorja M, Nahm MH, Hwang J. Low-cost, high-throughput, automated counting of bacterial colonies. Cytometry A. 2010; 77(8):790–7. Epub 2010/02/09. doi: 10.1002/cyto.a. 20864 PMID: 20140968. - NIST integrated counter

19. Bewes JM, Suchowerska N, McKenzie DR. Automated cell colony counting and analysis using the cir- cular Hough image transform algorithm (CHiTA). Physics

in medicine and biology. 2008; 53(21):5991– 6008. Epub 2008/10/07. doi: 10.1088/0031-9155/53/21/007 PMID: 18836215. - ChiTA

20. Geissmann Q. OpenCFU, a new free and open-source software to count cell colonies and other circular objects. PLoS One. 2013; 8(2):e54072. Epub 2013/03/05. doi: 10.1371/journal.pone.0054072 PONE- D-12-14509 [pii]. PMID: 23457446. - OpenCFU

21. Choudhry P (2016) High-Throughput Method for Automated Colony and Cell Counting by Digital Image Analysis Based on Edge Detection. PLoS ONE 11(2): e0148469. - IMJ Edge

22. Carpenter AE, Jones TR, Lamprecht MR, Clarke C, Kang IH, Friman O, et al. CellProfiler: image analy- sis software for identifying and quantifying cell phenotypes. Genome biology. 2006; 7(10):R100. Epub 2006/11/02. doi: 10.1186/gb-2006-7-10-r100 PMID: 17076895; PubMed Central PMCID: PMC1794559.

23. CellProfiler | Free open-source software for measuring and analyzing cell images. (2020). Retrieved 14 March 2020, from https://cellprofiler.org/